Journal of Biomedical Optics 7(1), 100–108 (January 2002)

Fiber-optical and microscopic detection of malignant tissue by use of infrared spectrometry

Uwe Bindig
Harald Winter
Laser- und Medizin-Technologie GmbH
Fabeckstrasse 60-62
14195 Berlin, Germany

Wolfgang Wäsche
Humboldt Universität Berlin
University-Hospital Charité
Schumannstrasse 20-21
10098 Berlin, Germany

Konstantinos Zelianeos
University of Athens
Faculty of Informatics
Department of Communications and Signal Processing
15784 Athens, Greece

Gerhardt Müller
Laser- und Medizin-Technologie GmbH
Fabeckstrasse 60-62
14195 Berlin, Germany
and
Freie Universität Berlin
University-Hospital Benjamin Franklin
Department of Medical Physics and Laser Medicine
Fabeckstrasse 60-62
14195 Berlin, Germany

Abstract. Several investigations were performed in order to develop an *in vivo* endoscopic method to differentiate between malignant and healthy tissue working on the assumption that each diseased state of biological tissue has its own characteristic infrared (IR) spectral pattern. The technical design of the laboratory setup is presented here together with the experimental details and the results. Two regions (1245–1195) and (1045–995) cm^{-1} within the fingerprint (<1500 cm^{-1}) region were selected for analysis. Lead salt diode lasers were used as excitation sources and IR radiation was transmitted via silver halide wave guides to the tissue to be investigated. The IR radiation is returned to a mercury–cadmium–telluride detector by another IR cable. The measurements were carried out in attenuated total reflectance and diffuse reflection/remission. Human colon carcinoma tissue, under humid conditions, was used as a target for experiments to simulate *in vivo* conditions. Specimens were mapped using a stepper, motor powered, $x/y/z$-translation stage with a spatial resolution of 1 μm. The results were compared with similar measurements from a Fourier transform IR (FTIR) interferometer/FTIR microscope setup in the wave number region of 4000–900 cm^{-1}. [DOI: 10.1117/1.1412439]

Keywords: ATR; remission; micro-FTIR; silver halide fiber; biomedical; lead salt diode laser; tissue.

Paper JBO-90027 received May 10, 1999; revised manuscript received Feb. 14, 2001; accepted for publication May 31, 2001.

1 Introduction

Several investigations to analyze the composition of biofluids, soft and hard tissue, using infrared (IR) spectroscopy as well as Raman spectroscopy were already reported.[1–5] For example, detailed IR investigations of the mineralization of hard tissue, such as bone, were made by Boskey et al.,[6] whereas extensive investigations using IR and/or microscope-FTIR spectroscopy have been carried out using human soft tissue (lenses,[7] atherosclerotic arteries,[8] breasts,[9] cervixex,[10] nails,[11] skin,[12] and colons[13]). Marked differences can be seen between the methods of sample preparation in terms of measuring the mode, parameters and conditions of sample preparation.

For clinical applications fiber based techniques are preferred. When light is transmitted to a waveguide or a crystal, most of the radiation transmitted is localized inside. But there is an evanescent wave that decays exponentially outside over a distance of a few wavelengths. If the IR fiber is in contact with a sample that has characteristic absorption lines the evanescent wave may be partially or totally absorbed. The total transmission of the fiber and the sample will decrease at these lines. Due to the long path length along the interphase sample/crystal or fiber surface multiple absorption processes take place. They can be used to determine the absorption of a sample in a nondestructive manner. The spectrum of the transmission losses is the basis of attenuated total reflectance (ATR) spectroscopy. ATR spectroscopy has been used for the study of materials in which intense scattering or absorption precludes transmission measurements. Only a few articles based on fiber-optic mid-IR spectrometry relate directly to the medical field. For example, Katzir and co-workers[14] designed a special measuring cell for an IR spectrometer equipped with a silver halide fiber to analyze blood serum; Butvina and co-workers[15] used IR fibers for the detection of melanoma and other skin diseases, whereas Bruch et al.[16] used Fourier transform infrared evanescent wave (FTIR-FEW) spectroscopy on tissue.

To enhance the sensitivity of the monitoring and control of chemical processes in liquids, gases and solids, Katzir and co-workers[17] used tunable IR diode lasers in combination with IR fiber optics. Pulsed IR diode lasers have also been used to create a diagnostic tool for sensitive detection of *Heliobacter pylorii* using an isotope ratio of $^{13}CO_2/^{12}CO_2$.[18]

We have focused our attention on the biomedical application of IR spectroscopy to detect changes within biological tissues, with the aim of designing an endoscopic device for use in minimally invasive medicine. This system will be combined with IR-imaging techniques using a focal plane array for rapid, safe, sensitive detection purposes.

The major nonorganic component of biological tissue is water, which has a high absorption in the infrared range. To minimize the influence of water on the IR spectra, in ATR mode a fiber-optic IR sensor should be carefully pressed onto the surface whereas in reflection mode either the surface of

Address all correspondence to Uwe Bindig, PhD. Tel: 49-30-8449-2326; Fax: 49-30-8449-2399; E-mail: u.bindig@lmtb.de

1083-3668/2002/$15.00 © 2002 SPIE

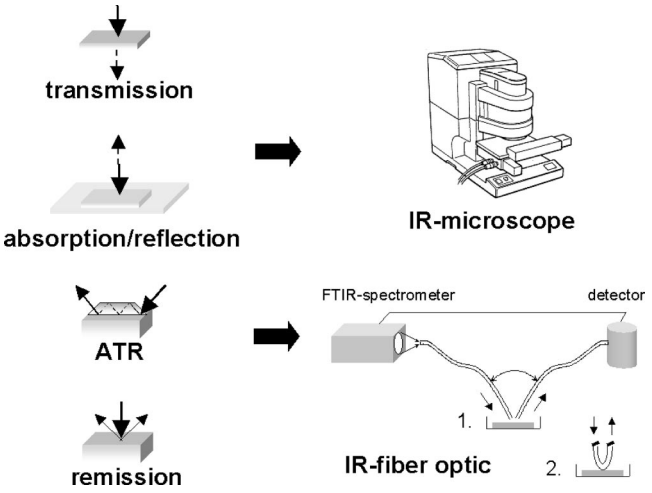

Fig. 1 Schematic of the IR measurement modes and the IR systems [fiber-optic measurements in noncontact (1) or contact (2) mode].

the tissue may be flushed with gas (steady state or pulsed) in order to dry the surface locally or alternatively a swab may be used to remove water.

Investigations with FTIR interferometers (fiber and microscope based; see Figure 1) on thin and thick specimens were carried out to determine specifications of the experimental setup using IR diode lasers. A description of the laboratory setup is given, together with preliminary results from the initial measurements. An analysis of the problems is shown and our current effort is focused on integrating the measurement equipment into an endoscopic device.

2 Material and Methods

Preliminary experiments were required before a laboratory setup for the investigation of human tissue using IR diode lasers could be established. Two FTIR interferometers (each series system 2000, Perkin-Elmer, Eden Prairie, MN) were used for this, one equipped with an IR microscope (AutoImage, Perkin-Elmer) including a charge coupled device (CCD) camera for the visible range and the other with an additional Raman port. The mercury–cadmium–telluride (MCT) detector of the microscope was used for recording spectra. Data analysis was performed by the Image Data Collection Software (Perkin-Elmer) and self-made software.

Polycrystalline silver halide fiber 700/900 of 1–1.5 m, with a numerical aperture (NA) of 0.6 (Infrared Fiber Sensors, Germany) was used for fiber-optic FTIR measurements. The fiber-optic device (Infrared Fiber Sensors) consisted of an optical coupler for the external port (IR lens: KRS-5, *f* 30-mm, *d*-40 mm) and a highly sensitive external pigtail MCT detector ($500\times500\,\mu m^2$) connected to an internal preamplifier. This system was connected to the FTIR spectrometer for signal processing and data evaluation.

2.1 Micro-FTIR Spectroscopy

Tissue specimens were made available by the Department of Pathology, University-Hospital Benjamin Franklin, Freie Universität Berlin, Germany. Fresh tissue samples were used without chemical fixation of the native structure and cryosectioning was performed using water instead of a freezing medium. For absorption/reflection measurements, nonstained 10 μm thin tissue sections were mounted on gold coated slides ($20\times20\,mm^2$; 1.5 μm Cr/200 μm Au, Fritz Haber Institute, Berlin, Germany). The specimens were stored in dry, darkened conditions at room temperature until these air-dried tissue sections were used for IR measurements. The stability of the IR spectra was confirmed periodically, and then with only slight shifts being observed in the signal intensity.

Drying of tissue leads to changes in the structure such as shrinkage, microrips, nonuniform thickness of the section (depending on the content of water in the original), sample surface roughness, and island or particle forming. Artifacts also occur as a result of the sections folding during cutting or transfer to the slide. A quality test for the tissue sections showed that the tissue layers remained mostly unaffected. This was confirmed by microscopic control after histological staining.

Native specimens of healthy and malignant tissue from the same patient were investigated. An initial assessment of parallel, thin hematoxylin-eosin (HE) stained tissue sections was carried out by a pathologist using standard histological parameters. The data obtained represent the basic information required for carrying out FTIR spectroscopy measurements. The native section was stained after IR mappings were complete to enable direct comparison with the resulting IR image.

The measurement was standardized for the mapping procedure, independent of mode, using the following parameters: a rectangular area was mapped on each sample using an aperture of $100\times100\,\mu m^2$, 64 scans were coadded; spectral range of 4000–900 cm^{-1}; resolution of 6 cm^{-1}; data interval of 2 cm^{-1}; apodization: filler. The background was scanned after every five points measured thus avoiding artifacts due to carbon dioxide or water vapor. A total of 900 IR spectra was collected for each map. For fiber-optic measurements, 512 or 1024 scans were coadded in the spectral range of 2200–800 cm^{-1}. The MCT detector linearity was tested with tissue phantoms (gelatin, Merck, Germany) prepared according to a standard procedure.

2.2 Reflection/ATR

The native tissue section thickness was set at >300 μm to avoid reflectance of IR radiation from a deeper interface or from the reverse side of the sample. A micro-ATR objective was used for the IR microscope measurements (germanium, area of contact $100\times100\,\mu m^2$, Perkin-Elmer). Even some select nonhuman tissue specimens were used for the fiber-optic ATR measurements.

3 Results and Discussion

3.1 Experiments with the FTIR Interferometers

3.1.1 *IR-Microscopic Measurements on Air-Dried Tissue Samples (Absorption/Reflection, Transmission)*

For transmission measurements using a distinct path length, soft tissue samples are either squeezed between transparent materials or homogenized at low temperature and filled into a precise measurement cuvette. In either case the microscopic structure of the tissue sample is disturbed. In order to avoid

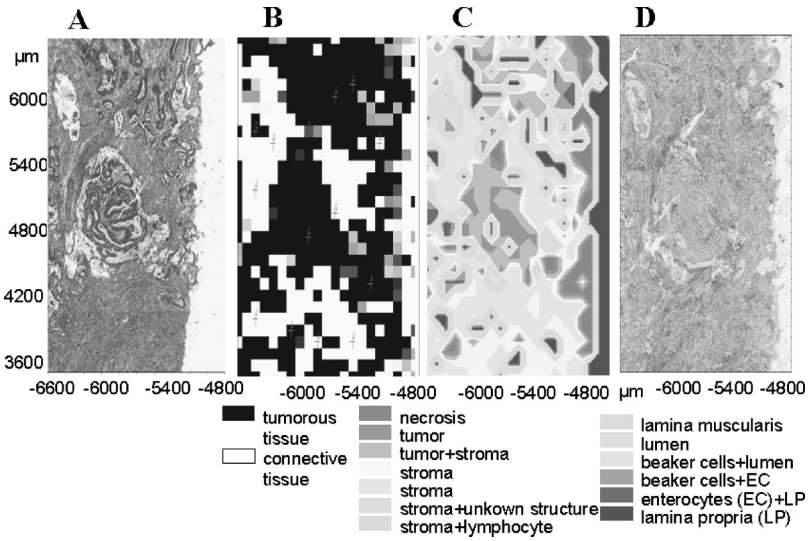

Fig. 2 (A) Visual microscopic image (IR microscope) of the HE-stained parallel 10 μm thin section (adenoma carcinoma of the colon). (B) IR map, intensity ratio of the second derivative at wave number ratio of 1223/1209 cm^{-1}, deduced from the original full spectra map. Due to the histological assessment this IR map is superimposed by the use of black and white squares to indicate tumor tissue (black) and connective tissue, (white), e.g., stroma. (C) Pseudocolored IR map, the result of image reconstruction using the correlation coefficient approach. For this the IR-mean spectra (second derivative, range of 900–1450 cm^{-1}) were built up for different types of tissue (see the legend for the color coded assignment). (D) Visual microscopic image (IR microscope) of the native 10 μm thin specimen (adenoma carcinoma of the colon) mounted onto a gold-coated slide.

mechanical alteration of the native tissue structure of colorectal cancer, cryosectioning was performed. In previous investigations done by our group, 10 μm thin tissue sections were mounted onto calcium fluoride slides and air dried at room temperature. Neither chemical fixation (e.g., formaldehyde or a freezing medium) nor whole tissue embedding methods were used because this leads to alteration of the microscopic tissue specific structure. Each step of the preparation procedure was carefully checked in order to get reliable and serious wave number ranges for tissue analysis.

The absorption/reflection measurement is a standard procedure for the investigation of thin layers, which can be mounted onto a variety of substrates. Gold is widely used as a reflective coating for investigations in the infrared region.[19,20] Using this method it has been possible to characterize the conformation of abnormal proteins found in pathological specimens of thin tissue sections of human origin.[19] To enhance the absorbance and the detection of sensitivity investigations of absorption/reflection were carried out using an IR microscope (high spatial resolution) and IR fiber-optic spectroscopy whereby the preparation of the samples differs from the methods given in the literature.[19,20]

The reliability of an infrared map is limited by several factors: by the system itself, by the measuring parameters and, more often than not, by the tissue quality. The sequence and results of a mapping experiment are shown in Figure 2. To avoid errors in data interpretation the infrared map and the IR map obtained were compared after analysis and mathematical conversion to the HE-stained parallel cryosection. For complete illustration, the native thin tissue section which was used for the IR microscopic mapping is shown in Figure 2(D).

Derivative techniques are of use for complex spectra and can enhance the sensitivity of the spectrum's outcome. Figure 2(B) shows the infrared map based on the intensity ratio of the second derivative at a wave number ratio of 1223/1209 cm^{-1}, deduced from the full spectra map. Due to the tissue's water content before drying and irregularities in tissue preparation normalization of the spectra is an essential step prior to quantitative analysis. Therefore the spectra were normalized in the fingerprint region (1590–900 cm^{-1}) for compensation of sample thickness. To simplify the illustration tumorous parts of the specimen are represented by closed squares, whereas nonaffected tissue appears colorless, which can be assigned mostly to connective tissue (e.g., stroma).

A second map was constructed from the initial one using the correlation coefficient analysis approach [Figure 2(C)]. For image construction of the tissue structure, discriminant analysis of more than two groups of spectra is necessary. In this case, all spectra (A) of a map are compared to a set of IR-mean spectra (second derivative, M_k) which correspond to a definitive type of tissue. Mixed states were even used in the analysis. For the assignments, pixels ($100\times100\ \mu m^2$) of the IR map were compared to the HE-stained tissue section. This allowed the corresponding IR spectrum to be correlated with the histological image (IR microscope). The unknown spectrum of the IR map is allocated to the mean spectrum, which results in the largest correlation coefficient. The correlation coefficient is used for definition of similarity:

$$\mathrm{corr}(A,M_k)=\frac{\int(A(v)-\langle A\rangle)[M_k(v)-\langle M_k\rangle]dv}{\sqrt{\int(A(v)-\langle A\rangle)^2dv\int(M_k(v)-\langle M_k\rangle)^2dv}}. \quad (1)$$

This results in a pseudocolored image which directly relates to the specimen characteristics. Comparison with the parallel histological section [the HE-stained image Figure 2(A)] shows a few mismatches caused by shrinkage, rupture or missing parts of the tissue. Although discriminant errors have not been analyzed quantitatively the coarse tissue structure is

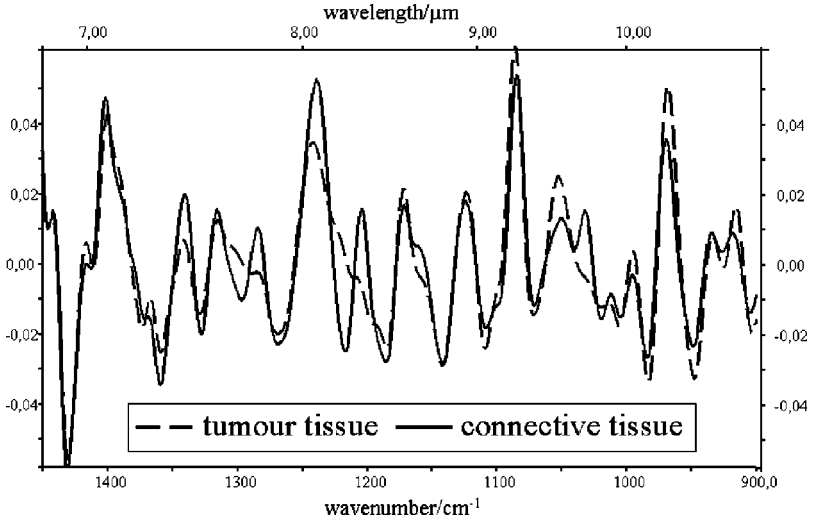

Fig. 3 FTIR-mean spectra of tumor and connective tissue (second derivative, range of 900–1450 cm^{-1}).

reproduced correctly. IR-mean spectra from the tumor and connective tissue (second derivatives, spectral range of 900–1450 cm^{-1}), which were used for the correlation coefficient analysis, are shown in Figure 3.

3.1.2 *IR Microscopic Measurements on Moist Tissue Samples*

Before starting IR-fiber-optic measurements, measurements were conducted with an IR microscope, keeping the samples moist, using remission and ATR. The main purpose of these experiments was to see if there was a significant wave number shift compared to the measurements on dry specimens. A measurement chamber was specially designed and tested for this purpose. Initially, it was not clear whether the specimens were subject to irreversible changes during IR measurement, e.g., cell lyses, a state that could subsequently influence the histological information obtained. However, subsequent histological staining and examination with the microscope showed little or no deterioration as a result of repeatedly conducting the standard procedure.

ATR spectroscopy. ATR measurements were made on thick, dry samples of colorectal tissue. In doing this it was possible to compare the results to equivalent measurements made in transmission mode. The penetration depth of the IR radiation was a limiting factor in this measurement procedure which was of the order of the IR radiation wavelength. The penetration depth can be increased by technical means such as the use of different optic materials or variation of the angle of incidence. The spectral information obtained is the result of a range of tissue components near the surface (mucus, epithelium). A contact method such as the ATR crystal has the additional disadvantage of contaminating the crystal, which affects its chemical resistance and requires cleaning after use, as well as a possible loss of cell material in the process. These problems can be partly solved by using inert materials (e.g., fibers with a diamond tip or a polymer coating in the contact area). Figure 4 shows the results of ATR measurements conducted with the IR microscope and IR fiber sensor on the same specimen.

The IR spectra of moist muscle tissue (bovine) recorded with the IR microscope and silver halide IR wave guides, respectively, show the typical intense absorption bands for proteins (amide-I and amide-II). The contact area of the tissue/ATR crystal for the IR microscope was 100 $\times 100\ \mu m^2$. However there is no way of controlling the exact size of the contact area or the pressure of the microcrystal on the soft tissue surface, which was mechanically stressed. The IR-sensor head, equipped with a disposable silver halide fiber (11 cm long, 700 μm in diameter) was connected to an excitation and emission waveguide. The sensing area (tissue/fiber)

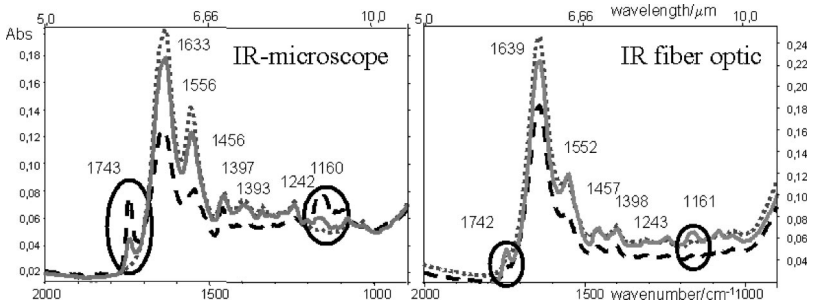

Fig. 4 Left: FTIR spectra obtained using an IR microscope: ATR mode, aperture $100\times100\ \mu m^2$, 300 μm thick muscle tissue (bovine). Right: Fiber-optic IR spectra (ATR mode, diameter of 700 μm), the sensor element was pressed onto the surface of fresh tissue (muscle, bovine).

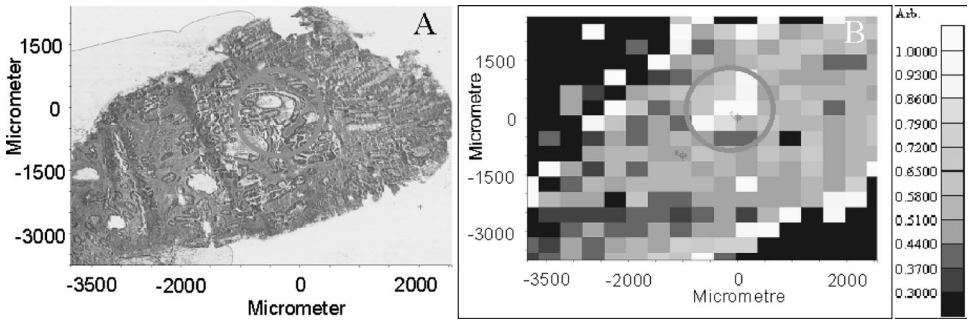

Fig. 5 Microphotograph (IR microscope) of (A) the HE-stained parallel 10 μm thin tissue section and (B) the IR reflection map according to KK conversion for the ratio of the wave number ranges of 1280–1185/1140–995 cm^{-1} from a 500 μm thick tissue sample (adenocarcinoma of the colon). For orientation the visual picture and the map was marked.

was approximately 7 mm^2. As a result minor shifts occur in the absorption maximum. After multiple measurements at the same position (time interval of approximately 2 min) additional absorption bands can be seen, for example, at 1743 and at 1160 cm^{-1}. This is partly due to the intensive contact which leads to a change in the contact area size (the roughness of the tissue surface due to wrinkles, microscopic gaps, etc.), and to a change in water content throughout the course of the measurement (displacement, drying). It results in more intense contact between the medium and the measurement device. The different absorption behavior in the contact area mainly leads to a change in the penetration depth of the IR radiation. As a consequence, the IR spectrum at any one measuring point can change over time. Micro-ATR measurements were carried out on the same native targets. Even the ratio of the intensity of the amide and the lipid absorption bands alters. This process is much more intense for micro-ATR measurements and occurs less frequently in measurements with IR fibers as a result of the large contact area.

However good resolution can be achieved with both ATR techniques using the IR interferometer in the range of 1400–1000 cm^{-1}, therefore making tissue differentiation possible.

Reflection spectroscopy. Systematic experiments using the IR microscope in remission to establish the penetration depth of IR radiation by the use of gelatin sections as a tissue phantom resulted in values of 250–300 μm. As a result, the investigations were conducted on moist tissue samples 500 μm thick to avoid any unwanted interference effects from the slide.

Representative results of one study are shown in Figure 5. Reflection measurements occur in a special measurement cell. The fresh, native, malignant tissue material was measured IR spectroscopically for 3, 24, and 72 h after sample preparation. The first measurement was carried out under moist conditions, whereby the sample was dry by the time the last measurement was made (not shown). To avoid the latent danger of biochemical alteration, the measurement time was reduced during measurements 1 and 2 by using a larger aperture ($400 \times 400\ \mu m^2$) with the result that spectroscopic information was averaged over a larger area of tissue.

For comparison, Figure 5(A) shows the counterpart to the thick tissue section which was taken before the mapping experiment—the microscope picture of the HE-stained 10 μm thin tissue section. The result of the mapping measurement is shown in Figure 5(B). The visual microscopic image (IR microscope), i.e., the histopathological information, was compared with the resulting full spectra map. The IR spectra were converted according to the Kramers–Kronig (KK) method and then combined onto an IR reflection map. The ratio of the wave number regions (1280–1185/1140–995 cm^{-1}) was evaluated. Only minor changes to the IR maps could be observed between the first and second measurements (3 and 24 h after sample preparation, respectively). The IR map of the same specimen made after 72 h shows changes to the tissue surface which are a result of effects caused by drying (not shown).

Visual inspection of the HE-stained specimen allows the tumorous parts to be differentiated. Even the result of the reconstructed IR map from the experimental data showed that differentiation between malignant tissue and other parts of the specimen is possible. In conclusion, the wavelength range chosen for the tissue differentiation in transmission can be transferred for measurements in remission mode.

Fiber-optic based laboratory setup. Before the ultimate aim of differentiating tissue using an endoscopic device could be achieved, it was essential to complete a fiber-optic based laboratory setup. The IR fiber was connected to the FTIR interferometer. Commercial silver halide fibers were used as the transmission material of choice because of their excellent physical properties with regard to transmission, numerical aperture, damping, flexibility and aging.

Description of laboratory setup. Coupling of the IR radiation was carried out by a closed unit connected to the interferometer with either a preadjusted KRS 5 lens system or a ZnSe lens. On the excitation side, an IR waveguide ($L = 1.5$ m, $d = 700\ \mu$m) was prepared on both ends with a Ti-SMA switch. An external MCT pigtail detector was used (active detector area of $500 \times 500\ \mu m^2$; Infrared Fiber Sensors, Germany) on the detection side. A permanent fiber/detector coupling ($L = 1.8$ m, $d = 700\ \mu$m, Ti-SMA switch) was fitted on the detector side by a silver halide microlens. The sample compartment is shown Figure 6.

Results: Preliminary experiments were carried out. An example will be explained in detail. The moist tissue material was examined with both the fiber-optic based laboratory setup and the IR microscope. The following results were obtained. Just for documentation purposes, the visual microscopic image of the native, moist 300 μm thick tissue section was prepared by the IR microscope [Figure 7(A)]. Then an IR map

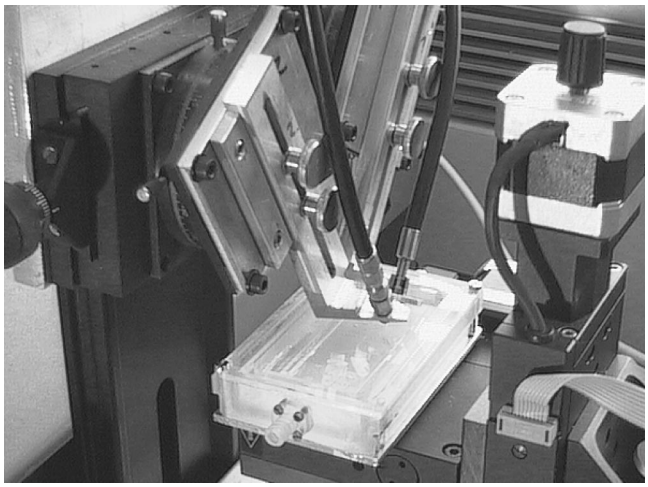

Fig. 6 View of the sample compartment and the fiber-optic based laboratory setup.

(remission mode) of a restricted area of the tissue section was recorded. On the basis of these data, and in accordance with the previously successful KK conversion, a pseudocolor map was made for the area ratios of the wave number region (1280–1185/1140–995 cm^{-1}) using the converted IR-spectral data. The recorded reflection spectra of the ''*L*'' marked regions after KK conversion are shown in Figure 7(B). These spectra can be compared with the fiber based measurements that were carried out on the same tissue sample [Figure 7(C)]. IR fibers with a diameter of 700 μm were used. Optimal results were obtained using an experimental setup in which both the excitation and detection fibers had an angle of incidence of 60° to each other. The fiber to tissue distance was approximately 0.5 mm. A gold standard background was recorded every 10 measuring points, analogous to the IR microscopic measurements. Taking the spectral characteristics of the IR fibers into account, the fiber-optic based IR map that resulted from the previously described data processing [the ratio of the wave number regions (1262–1130/1103–972 cm^{-1})] corresponds well with the IR microscopic result. Areas without color in the IR map are assigned to the slide material.

Representative reflection spectra are shown in Figures 7(B) and 7(C). The wave number regions are marked separately for spectroscopic differentiation in the IR map.

It should be emphasized that the results (reflection mode tissue spectra) of a fiber based laboratory setup using an IR interferometer as the excitation source can be compared to the IR microscope results using moist tissue samples. The spectral information allows differentiation between healthy/malignant tissues. Moreover, from the results, the wave numbers for colorectal tissue differentiation could be verified compared to the IR measurements on dry tissue specimens. This aided in the choice of suitable IR diode laser for the experimental laboratory setup.

3.2 Experiments with IR Diode Lasers

3.2.1 *Experimental Setup with IR Diode Lasers as the Excitation Source*

Experiments using a lead salt diode laser were realized according to the schematic diagram shown in Figure 8.

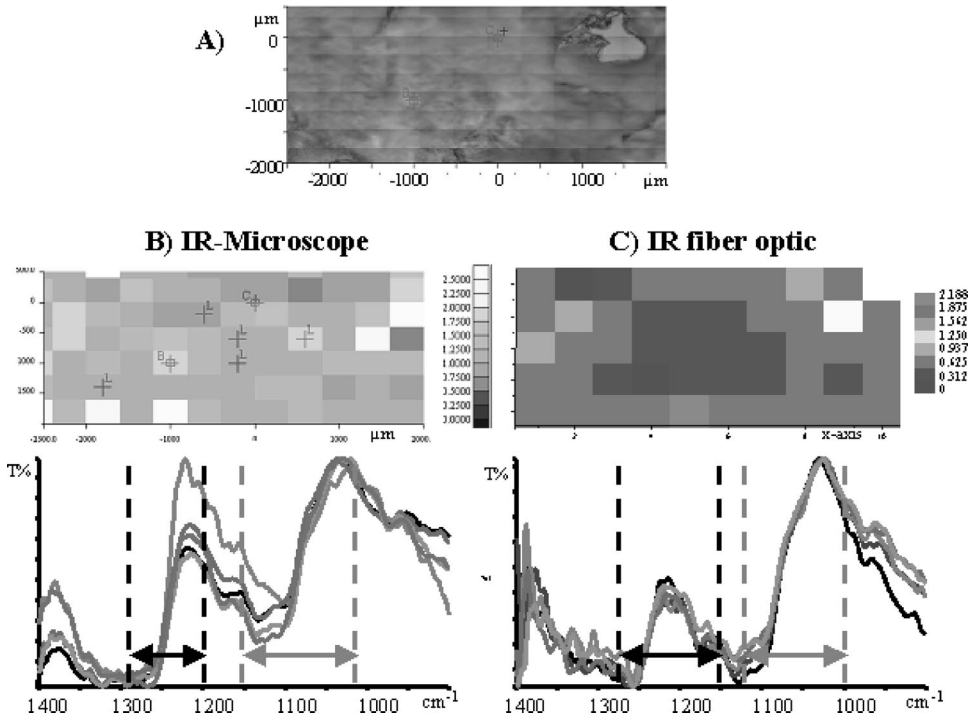

Fig. 7 (A) Visual microscopic image of a 300 μm thick, native, moist specimen (adenocarcinoma of the colon). (B) IR microscope: Pseudocolored IR map (aperture 400×400 μm^2) after KK conversion and IR reflection spectra, which correspond to the positions marked on the map. The wavelength region used for analysis is marked on the spectra. (C) IR fiber optic: Pseudocolored IR map and a number of corresponding IR reflection spectra after KK conversion that were used for construction of the reflection map. The wavelength range used for analysis is marked on the spectra.

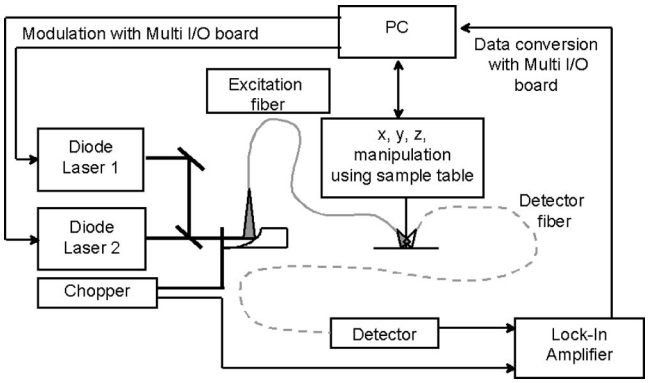

Fig. 8 Schematic diagram of the fiber-optic based laboratory setup using lead salt diode lasers.

For the laboratory setup two high power multimode lead salt diode lasers (Mütek Infrared Systems, Germany) were used as the IR-excitation source [diode 1: 995–1045 cm^{-1} (9569–10 050 nm)], [diode 2: 1145–1245 cm^{-1} (8032–8733 nm)]. The bandwidth is between 20 and 30 cm^{-1}. The usable wavelength range is approximately 50 (diode 1) and 100 cm^{-1} (diode 2). The actual wavelength depends on the diode current. The current is modulated at the laser driver in order to scan the wavelength range. After being collimated with spherical concave mirrors, both IR beams are overlapped and are then coupled into a fiber using another spherical concave mirror. The IR fiber and the MCT detector are described above. The signal at the detector is evaluated using a lock-in amplifier (model SR830, Stanford Research Systems, CA). To position the sample and to record a map, a translation stage with three axes is set up which moves the sample underneath the fixed IR fibers and is controlled by a PC. The resolution in either direction is 1 μm.

To evaluate the setup of the IR diode lasers, the recorded spectra were compared with the spectra of the FTIR interferometer. The results cannot be compared directly because the excitation sources differ. The interferometer may use a Nernst glowing bar which can be regarded as blackbody radiation.

The diode lasers emit at different modes while the diode current is scanned. This means that the spectral emission has to be taken into account at every wavelength in order to obtain a spectrum that is comparable with the spectrum from the FTIR interferometer. Deconvolution of the IR spectra is not necessary because the differentiation of tissue requires only the detection of relative differences.

3.2.2 *Results*

Figure 9 shows preliminary results from thick, moist normal and malignant colorectal tissue specimens. The tissue area was scanned point to point in rows. Each point represents the raw data and the data normalized to the gold standard. All spectra of the raw data show almost the same course, the main differences being in intensity. From the index point 140 differences occur. Differences can be clearly seen between the spectra of normal and malignant tissue where diode laser 2 is the excitation source. Not only are there differences in intensity but also additional signals. The high level of noise in the normalized spectra is due to the low intensity of the excitation sources.

The initial results indicate that measurements using IR diode lasers and moist tissue samples are possible and that typical tissue differences can also be detected. This proves, in

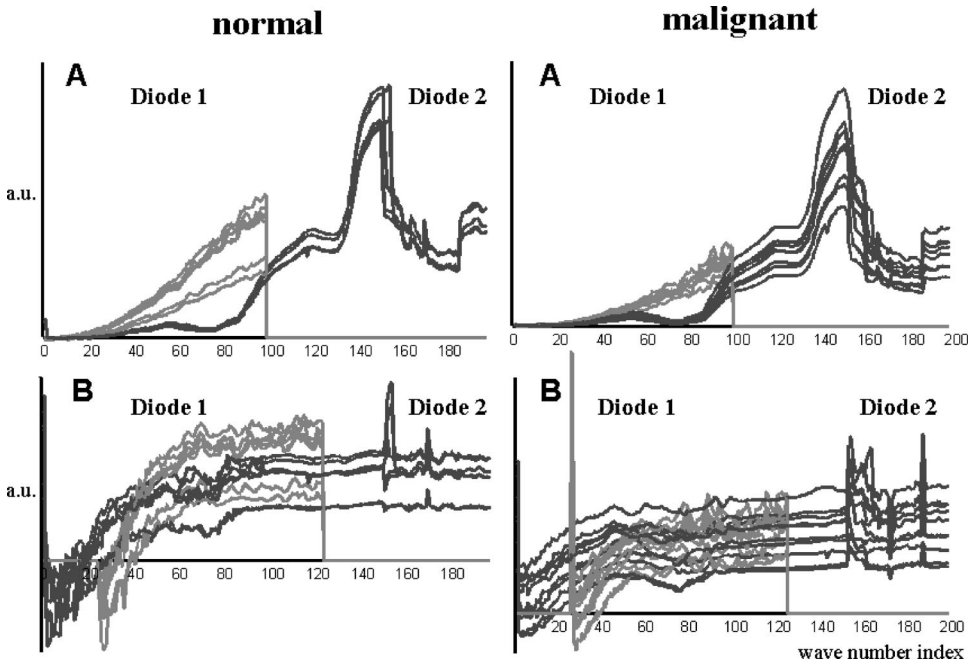

Fig. 9 Preliminary results from measurements using IR diode lasers on moist, normal and malignant tissue samples. Each spectrum equals one measuring point on the tissue. (A) Raw data of normal (left) and malignant (right) tissue. (B) Data normalized to the gold standard of normal (left) and malignant (right) tissue.

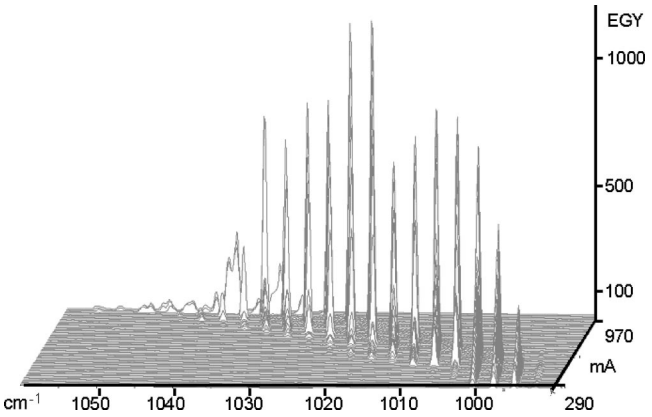

Fig. 10 Three-dimensional view of the FTIR spectra to characterize IR laser diode 1.

principle, the feasibility of this measurement method. The measurement time could be further reduced by optimizing the conditions.

3.3 Characterization of the Diode Lasers

As stated earlier, it is not usually necessary to know the exact spectra of the diode lasers in order to differentiate tissue. However, because comparison of the different excitation sources allows the evaluation of their individual benefits, we chose to determine the spectra of the diode lasers. This was carried out using the FTIR interferometer with the Raman port. The Raman port was detached in order to couple the IR diode lasers to this port. In this way the radiation takes almost the exact same path as the internal IR radiation source.

The resolution of the interferometer was set to 0.5 cm^{-1} and single beam spectra were recorded. One scan per spectrum was sufficient for a significant signal to noise ratio. First the spectrum of the internal source was recorded (not shown). The spectra of the diode lasers are recorded using the same settings to allow comparison with each other.

Figure 10 shows a three-dimensional plot of the spectra recorded with diode 1. The preadjusted temperature was 95 K and the spectra recorded started with the current at the laser threshold and continued to its maximum setting. The spectrum was recorded with a spacing of 10 mA. The *x* axis shows the wave number region, the *y* axis, the adjusted current and the *z* axis, the intensity. The diode emits in the range desired between 995 and 1045 cm^{-1} and its intensity is over 20 times greater than that of the internal IR source of the FTIR interferometer. It should be noted that the individual modes are slowly turned on at certain currents and become weaker as the current is increased. This process does not have any effect on the position of the mode. This means there is no change in the wave number when the current is changed. The only change occurring is in the intensity of the mode.

The settings for diode 2 are the same as those for diode 1. The only difference is that the spacing between two spectra is 100 instead of 10 mA. The reason for this is that diode 2 does not show the radiation features desired and therefore numerous measurements were made to determine how close diode 2 gets to the specifications determined. The intensity is much weaker than that of diode 1 (not shown) and the wave number region for diode 2 is out of range: 1140–1200 instead of 1145–1245 cm^{-1}.

4 Conclusion

Absorption/reflection as well as ATR and remission techniques (IR microscope and IR fiber optic) were applied using either thin or thick specimens of healthy and malignant human colorectal tissue. IR measurements in transmission mode were already done in previous investigations. This work indicated that IR spectroscopy could prove to be a powerful tool for tissue characterization. It is true that there are potential pitfalls, particularly in the sample preparation procedure, the parameter for measurement itself and data analysis. Nevertheless it is likely that fiber-optic ''mapping'' could be done on tissue and that this mapping *in vivo* would make it possible to distinguish between healthy and malignant tissue. Additional IR spectroscopic investigations are in progress for more detailed analysis with an eye toward IR fiber handling and minimizing the influence of water (absorbance) by technical means.

Although tissue differentiation seems to be possible with the current experimental laboratory setup using IR diode lasers as excitation sources and IR silver halide fibers for radiation transmission, for routine measurements certain portions of the measurement method require further optimization. Using the method described here for characterizing IR diode lasers would make selection of suitable diodes and developing an algorithm for evaluating the signal measured more feasible. The scientific knowledge gained from this work could be used to design an endoscopic device into which the facility for measurement is integrated.

Acknowledgment

This work was supported by the German BMBF, Project No. 13N7064.

References

1. S. E. Cope, T. L. Freeman, B. J. Rembacken, M. R. Stringer, D. N. Batchelder, and S. B. Brown, ''The analysis of human colon tissue using Raman spectroscopy,'' *Proc. SPIE* **3197**, 110–114 (1997).
2. A. Mahadevan-Jansen and R. Richards-Kortum, ''Raman spectroscopy for the detection of cancers and precancers,'' *J. Biomed. Opt.* **1**, 31–70 (1996).
3. D. Pappas, B. W. Smith, and J. D. Winefordner, ''Raman spectroscopy in bioanalysis,'' *Talanta* **51**, 131–144 (2000).
4. R. G. Zhbankov, S. P. Firsov, E. V. Korolik, P. T. Petrov, M. P. Lapkovski, V. M. Tsarenkov, M. K. Marchewka, and H. Ratajczak, ''Vibrational spectra and the structure of medical biopolymers,'' *J. Mol. Struct.* **555**, 85–96 (2000).
5. E. B. Hanlon, R. Manoharan, T.-W. Koo, K. E. Shafer, J. T. Motz, M. Fitzmaurice, J. R. Kramer, I. Itzkan, R. R. Dasari, and M. S. Feld, ''Prospects for *in vivo* Raman spectroscopy,'' *Phys. Med. Biol.* **45**, R1–R59 (2000).
6. R. Mendelsohn, E. P. Paschalis, and A. L. Boskey, ''Infrared spectroscopy, microscopy, and microscopic imaging of mineralizing tissues: Spectra–structure correlations from human iliac crest biopsies,'' *J. Biomed. Opt.* **4**, 14–21 (1999).
7. Y. Ozaki, F. Kaneuchi, T. Iwamoto, M. Yoshiura, and K. Iriyama, ''Non-destructive analysis of biological materials by FTIR-ATR. Method I: Direct evidence for the existence of collagen helix structure in lens capsule,'' *Appl. Spectrosc.* **43**, 138–141 (1989).
8. D. R. Kodall, D. M. Small, J. Powell, and K. Krishnan, ''Infrared micro-imaging of atherosclerotic arteries,'' *Appl. Spectrosc.* **45**, 1310–1317 (1991).

9. M. Meurens, J. Wallon, J. Tong, H. Noel, and J. Haot, ''Breast cancer detection by Fourier transform infrared spectrometry,'' *Vib. Spectrosc.* **10**, 341–346 (1996).
10. H. Fabian, M. Jackson, L. Murphy, P. H. Watson, I. Fichtner, and H. H. Mantsch, ''A comparative infrared spectroscopic study of human breast tumors and breast tumor cell xenografts,'' *Biospectroscopy* **1**, 37–45 (1995).
11. M. G. Sowa, J. Wang, C. P. Schultz, M. K. Ahmed, and H. H. Mantsch, ''Infrared spectroscopic investigation of *in vivo* and *ex vivo* human nails,'' *Vib. Spectrosc.* **10**, 49–56 (1995).
12. P. T. T. Wong, S. M. Goldstein, R. C. Grekin, T. A. Godwin, C. Pivik, and B. Rigas, ''Distinct infrared spectroscopic patterns of human basal cell carcinoma of the skin,'' *Cancer Res.* **53**, 762–765 (1995).
13. B. Rigas, S. Morgello, I. S. Goldman, and P. T. T. Wong, ''Human colorectal cancers display abnormal Fourier-transform infrared spectra,'' *Proc. Natl. Acad. Sci. U.S.A.* **87**, 8140–8144 (1990).
14. Y. Gotshal, R. Simhi, B.-A. Sela, and A. Katzir, ''Blood diagnostics using fiberoptic evanescent wave spectroscopy and neural networks analysis,'' *Sens. Actuators B* **42**, 157–161 (1997).
15. N. I. Afanasyeva, S. Kolyakov, and L. N. Butvina, ''Remote skin tissue diagnostics *in vivo* by fiber optic evanescent wave Fourier transform infrared (FEW-FTIR) spectroscopy,'' *Proc. SPIE* **3257**, 260–266 (1998).
16. R. F. Bruch, S. Sukuta, N. I. Afanasyeva, S. F. Kolyakov, and L. N. Butvina, ''Fourier transform infrared evanescent wave (FTIR-FEW) spectroscopy of tissue,'' *Proc. SPIE* **2970**, 408–415 (1997).
17. D. Bunimovich, R. Kellner, R. Krska, A. Mesica, I. Paiss, U. Schiesl, M. Tacke, K. Taga, and A. Katzir, ''A system for monitoring and control of processes based on IR fibers and tunable diode lasers,'' *J. Mol. Struct.* **292**, 125–132 (1993).
18. B. Schommartz, M. Haisch, and P. Hering, ''IR-diodenlaser-spektroskopie zur bestimmung von Isotopenverhältnissen in CO_2,'' *Isotopenpraxis Environ. Health Stud.* **30**, 271 (1994).
19. L. S. Lee, S. Y. Lin, C. W. Chi, H. C. Liv, and C. L. Cheng, ''Non-destructive analysis of the protein conformational structure of human pituitary adenomas using reflectance FTIR microspectroscopy,'' *Cancer Lett. (Shannon, Irel.)* **94**, 65–69 (1995).
20. T. J. O'Leary, W. F. Engler, and K. M. Ventre, ''Infrared microspectroscopy of human tissue,'' *Appl. Spectrosc.* **43**, 1095–1097 (1989).